Supporting Information

Aoyama *et al.* 10.1073/pnas.0806391106

SI Text

Absorption Spectral Measurement for Single Crystals of Cytochrome *c* Oxidase. The X-ray diffraction goniometer in BL44XU at the SPring-8 was equipped with an absorption spectrophotometer to measure absorption spectra of the single crystals under X-ray exposures, as outlined in Fig. S1. The measuring visible light beam was injected into a single crystal placed in the X-ray goniometer perpendicularly to the X-ray beam under a cryostream of N_2 at 100 K. The measuring light beam was focused to a diameter of ≈50 μm. The most-extended plane (010) of the CcO crystal (≈500 × 500 μm) was placed perpendicularly to the measuring visible light beam. The X-ray beam size without the slit system for X-ray diffraction experiments was large enough for irradiation of the entire space exposed to the measuring visible light beam in the crystal. A multichannel detector was equipped for monitoring the real-time spectral changes. The measuring light was guided by optical fibers, which enable the spectrophotometer to be placed in a limited space near the goniometer in the X-ray diffraction beam line. The system shown in Fig. S1 is for examination of the effects of X-ray irradiation on the absorption spectra of any protein crystal without performing X-ray diffraction experiments. The spectrophotometer was custom designed and installed. All of the parts of the spectrophotometer required for the installation are commercial products. The details of the spectrophotometer are available upon request.

X-Ray Diffraction Experiments. All of the X-ray experiments were carried out at BL44XU of the SPring-8. The beamline was equipped with an image plate detector, DIP4040. The X-ray beam cross-section for X-ray diffraction experiments was 50 × 50 μm, and the wavelength was 0.9 Å. The photon flux density was ≈2×10^{14} photons s^{-1} mm^{-2}. Crystals of ≈500 × 500 × 200 μm were selected for the experiments. All experiments were performed at 100 K. Intensity data were processed by the CCP4 program MOSFLM (1) and scaled by using SCLONE (2), which was developed by us for diffraction images with no serial oscillation angle.

Structural Analyses. The initial phase angles of structure factor up to 5-Å resolution were obtained by the molecular replacement (MR) method using the fully oxidized "as-isolated" structure previously determined at 1.8-Å resolution (PDB ID code 2DYR) (3). Phase extension to the highest resolution of each data set was carried out by density modification coupled with noncrystallographic symmetry averaging using the CCP4 program DM (4), and the resultant phase angles ($\alpha_{MR/DM}$) were used to calculate electron density maps (MR/DM maps) with Fourier coefficients of $F_O\exp(i\alpha_{MR/DM})$. Structural refinement was carried out by using X-PLOR (5) and REFMAC (6). After several rounds of refinement and manual remodeling, bulk solvent correction and anisotropic scaling of the observed and calculated structure factor amplitudes were incorporated into subsequent rounds of refinement. The anisotropic temperature factors for iron, copper, and zinc atoms were imposed on the calculated structure factors. The quality of the structural refinement was examined by calculation of the R and free R values (7). Several water molecules that were clearly identified in MR/DM map were not included in the structure refinement, to compare their peak heights as reference peaks with the peak height between Fe_{a3} and Cu_B in the (Fo-Fc) difference Fourier map. When 2 (Fo-Fc) maps with different data sets were compared with each other, the maps were calculated at the lower resolution, to reduce the difference between 2 maps resulting from differences in quality; the map for the data set with the lower averaged B-factor was broadened by calculating the Fourier summation with the coefficient of (Fo-Fc) $\exp(i\alpha_C)$ $\exp(-\Delta B \sin^2(\theta/\lambda))$, where ΔB represents the difference of averaged B-factors between 2 datasets.

Effect of Excessive X-Ray Irradiation on the Structure of the O_2 Reduction Site. An (Fo-Fc) map for the 405- to 594-s dataset was calculated at 1.95-Å resolution. This difference map given in Fig. S2 shows that an electron density peak appeared near the hydroxide group of Tyr-244. The (Fo-Fc) difference electron density map together with the (Fo-Fo) difference maps indicates that a water molecule generated by reduction of the peroxide was transferred to Tyr-244 to form a hydrogen bond with the hydroxyl group of Tyr-244.

Statistics of X-Ray Structural Analyses. Statistics of intensity datasets and structural refinements for the 1- and 15-s exposure experiments are given in Table S1. Statistics of peak heights of the electron densities between Fe_{a3} and Cu_B are listed in Table S2. The refinement statistics for X-ray structural analyses performed for examination of the effect of excessive X-ray irradiation are given in Table S3.

1. Leslie AGW (1992) Recent changes to the MOSFLM package for processing film and image plate data. *Jnt CCP4 ESF-EAMCB Newslett Protein Crystallogr* 26.
2. Hirata K, *et al.* (2004) Scaling of one-shot oscillation images with a reference data set. *J Synchrotron Rad* 11:60–63.
3. Shinzawa-Itoh K, *et al.* (2007) Structures and physiological roles of 13 integral lipids of bovine heart cytochrome *c* oxidase as the driving element of the proton-pumping process. *EMBO J* 26:1713–1725.
4. Cowtan K (1994) 'dm': An automated procedure for phase improvement by density modification. *Jnt CCP4 ESF-EACBM Newslett Protein Crystallogr* 31:34–38.
5. Brünger A, Kuriyan J, Karplus M (1987) Crystallographic *R* factor refinement by molecular dynamics. *Science* 235:458–460.
6. Winn M, Isupov M, Murshudov GN (2001) Use of TLS parameters to model anisotropic displacements in macromolecular refinement. *Acta Crystallogr D* 57:122–133.
7. Brünger AT (1992) Free *R* value: A novel statistical quantity for assessing the accuracy of crystal structures. *Nature* 355:472.

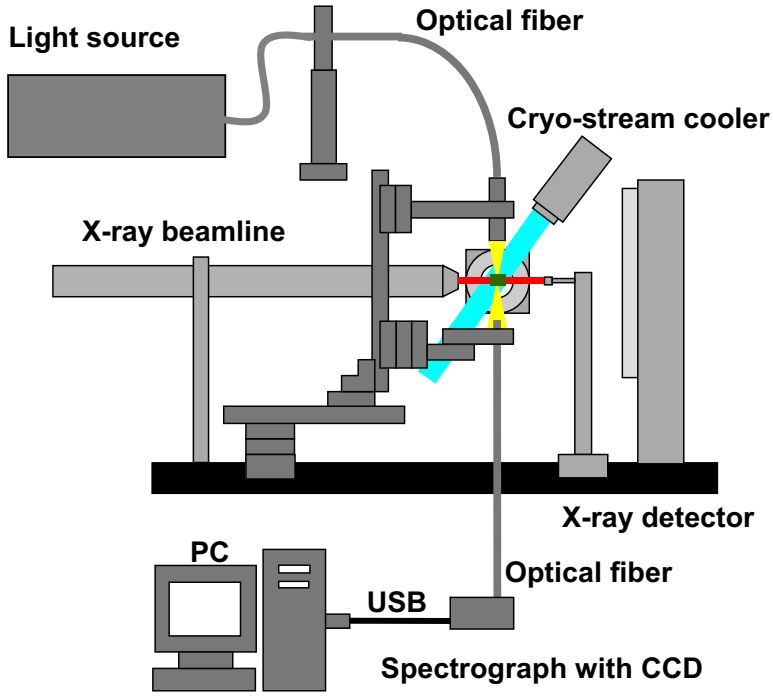

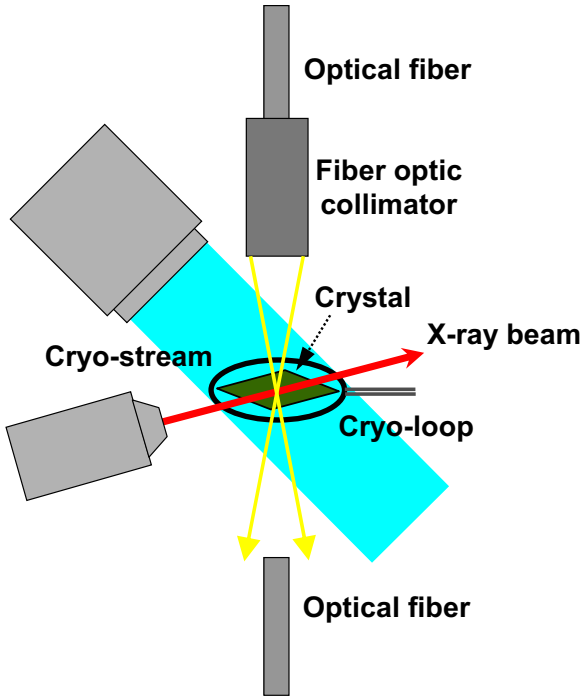

Fig. S1. Block diagram for absorption spectral measurement system for measurement of single crystals. Blue, N_2 stream at 100 K; yellow, the measuring visible light beam; red, X-ray beam from the synchrotron beam line. The lower illustration is a close-up of the arrangement for setting a crystal to be examined.

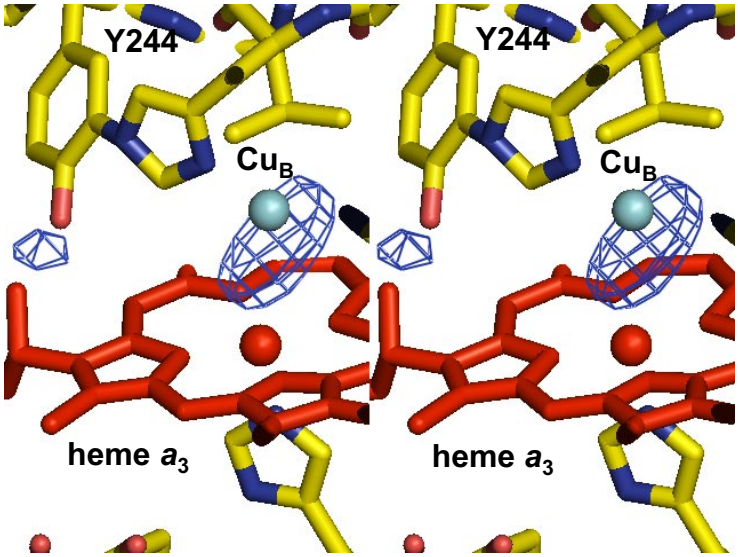

Fig. S2. (*Fo-Fc*) difference electron density map in stereoview for the 407- to 594-s data, calculated at 1.95-Å resolution. Electron density cages for the electron density between and Fe_{a3} and Cu_B and for a water molecule hydrogen-bonded to Tyr-244 are depicted at the 5σ level in a stick model around the O_2 reduction site. Carbon, nitrogen, and oxygen atoms are colored in yellow, dark blue, and red, respectively. Heme a_3 and Cu_B are represented in red and green

Table S1. Statistics of intensity data and refinements

Exposure time, s	1	15
No. of images	281	308
No. of crystals	190	201
Diffraction data		
Resolution, Å	56.80–2.50 (2.65–2.50)	56.80–2.10 (2.21–2.10)
Observed reflections	1,215,123 (76,914)	2,867,365 (342,596)
Independent reflections	216,525 (24,186)	390,624 (56,364)
I/σ (I)	2.8 (1.4)	3.9 (1.7)
Averaged redundancy*	5.6 (3.2)	7.3 (6.1)
Completeness, %	92.0 (92.0)	99.2 (98.8)
R_{merge}†, %	20.0 (44.3)	12.9 (39.5)
Refinement		
Resolution, Å	40–2.50	40–2.10
R‡, %	18.5	17.6
R_{free}§, %	23.3	21.0
R.m.s. deviation¶, bonds, Å	0.021	0.033
R.m.s. deviation¶, angle, °	2.1	2.6

*Redundancy is the number of observed reflections for each independent reflection.

†$R_{merge} = \Sigma_h \Sigma_j |I(h,j) - \langle I(h)\rangle| / \Sigma_h \Sigma_j |I(h,j)|$, where $I(h,j)$ is the intensity value of the jth measurement of h, and $\langle I(h)\rangle$ is the corresponding mean value of $I(h)$ for all j measurements.

‡$R = \Sigma_h ||Fo(h)| - |Fc(h)|| / \Sigma_h |Fo(h)|$, where $Fo(h)$ and $Fc(h)$ are the observed and the calculated structure factors of h, respectively.

§R_{free} is the free R factor evaluated for the 5% of reflections that are excluded from the refinement.

¶R.m.s. deviation from the corresponding ideal structures.

Table S2. Electron density of peroxide and selected water molecules

Electron density, $e^{-}/Å^3$	1-s exposure	15-s exposure
OO	0.51	0.59
Waters*		
2,007	0.25	0.28
2,014	0.38	0.41
2,039	0.32	0.38
Averaged	0.31	0.35
OO/water ratio	1.64	1.67
$\sigma^{\dagger}$, $e^{-}/Å^3$	0.044	0.043

*Three water molecules were not included in the structural refinement (to compare their electron densities with that of peroxide).
†R.m.s. deviation from the averaged value of the electron density.

Table S3. Intensity data and structural refinement at 100 K

Parameter	1st.	2nd	3rd
Exposure time, s	9–198	207–396	405–594
Diffraction data			
Resolution, Å	200–1.95 (2.02–1.95)	200–1.95 (2.02–1.95	200–1.95 (2.02–1.95)
Observed reflections	1,955,994 (129,337)	1,939,157 (127,101)	1,909,701 (123,760)
Independent reflections	473,853 (44,790)	471,994 (44,125)	469.353 (43,512)
I/σ (I)	7.9 (1.1)	7.9 (1.1)	8.0 (1.0)
Averaged redundancy	4.1 (2.9)	4.1 (2.9)	4.1 (2.8)
Completeness, %	96.8 (92.1)	96.4 (90.8)	95.8 (89.5)
R_{merge}, %	5.9 (29.6)	5.9 (29.3)	5.6 (29.6)
Refinement			
Resolution, Å	40–1.95	40–1.95	40–1.95
R, %	18.1	18.2	18.3
R_{free}, %	21.4	21.4	21.6
R.m.s. deviation, bonds, Å	0.030	0.029	0.029
R.m.s. deviation, angle, °	2.790	2.766	2.751

The definitions are the same as in Table S1.